Effects of Surface Active Agents on Mass Transfer during Droplet Formation, Fall, and Coalescence

This experimental study shows effects of anionic and cationic surface active agents on mass transfer during drop formation, fall, and coalescence for both continuous and disperse phase-controlled systems. Three dispersion nozzles, mounted with 1.906 cm equilateral pitch, and a 5.08 cm I.D. extraction column were used to simulate certain conditions in commercial liquid-liquid extraction units.

The surfactant effects on extraction were pronounced, frequently reducing transfer to 10% of that in uncontaminated systems, with marked minima at intermediate concentrations of surfactant. In contrast, the continuous phase coefficient during coalescence was substantially increased by surfactants, with maxima in some cases.

A. H. P. SKELLAND and C. L. CAENEPEEL

University of Notre Dame
Notre Dame, Indiana

SCOPE

The frequent presence of trace amounts of surface active contaminants in commercial extraction equipment is by now widely recognized. The effects of these materials in distorting performance from that predicted by many studies with pure systems (*28* to *52*) must eventually be accommodated. In 1939 Sherwood et al. (9, 10) showed that up to 40% of the total extraction may occur during the important stages of drop formation and coalescence. Despite these well-known considerations, the present paper is apparently the first study of the effects of surface active agents on extraction during drop formation and coalescence.

Many investigators (*1* to *14*) have reported a reduction in mass transfer for systems containing surface active substances. These materials can be surfactants, impurities, plasticizers from tubing used in the equipment (*9*), or metallic colloids from pipes and fittings. The effects of surface active agents (S.A.A.) on mass transfer across an interface may be placed in two categories:

1. They may form an interfacial barrier of a mechanical, physical, or chemical nature (*3*, *8*, *9*, *15*), and

2. they may modify the relevant hydrodynamics by reducing the rate of internal circulation in drops (*4*, *10*, *76*, *77*), damping the interfacial waves or oscillations (*2*, *13*, *17*, *18*, *72*), decreasing the terminal velocity of drops (*1*, *2*, *4*, *17* to *24*), lowering the interfacial tension (*19*, *24* to *27*), lessening the transmission of turbulence across the interface (*16*), and retarding the rate of coalescence (*85*, *87*).

Mathematical models of the effects of surface active agents on mass transfer from drops are developed by Huang and Kintner (*53*) and by Lochiel (*54*), who employed equations presented by Chao (*55*). Davies (*56*) extended a theory due to Levich (*57*, *58*) to describe the effect of small amounts of surface active materials on mass transfer across a gas-liquid interface into a turbulent liquid.

The present study simulates operation in common forms of extraction equipment by use of multiple nozzles and plane coalescence areas per droplet stream which are similar to those used commercially. Surfactants are both cationic and anionic, and the systems are either continuous or disperse phase controlled.

CONCLUSIONS AND SIGNIFICANCE

The effects of trace amounts of surfactants on all three stages of the process—drop formation, fall, and coalescence—is pronounced, both for the continuous and dispersed phases. Many of the results exhibit a dramatic reduction in the mass transfer coefficient with increasing S.A.A. concentration. For the disperse phase-controlled system, transfer rates in all three stages may be reduced by either anionic or cationic S.A.A. to less than 10% of that in uncontaminated systems. Similar but less severe reductions were observed for both surfactants in the continuous phase-controlled system during formation and free fall. A notable feature is the frequent occurrence of a minimum in the coefficient at S.A.A. concentrations which are much less than the bulk values corresponding to interfacial saturation in static systems. This phenomenon is tentatively linked to the optimum concentration of soluble S.A.A. often found to give maximum damping of waves on a free liquid surface (*72*).

In contrast, the continuous phase coefficient during coalescence was substantially increased by surfactants, with maxima at intermediate concentrations of S.A.A. in the case of the cationic agent. An explanation is offered in terms of extended surface due to retarded coalescence of the drops for these systems.

Correspondence concerning this paper should be addressed to A. H. P. Skelland at the University of Kentucky, Lexington, Kentucky. C. L. Caenepeel is at the California State Polytechnic College, Pomona, California.

The effect of increasing the time of drop formation t_F on the ratio of mass transfer coefficients with and without surfactants is in most cases consistent with the suppression of interfacial movement by the S.A.A. This induces a mass transfer mechanism closer to the penetration theory based on t_F during both formation and coalescence, with a smaller dependence on formation time than found in the absence of surfactants.

In several cases, results are compared with theoretical predictions which make no allowance for effects of S.A.A. Correlation could not, therefore, be expected, but it is felt that order-of-magnitude comparisons might be of some interest. Certainly some such estimates will ultimately be needed for design guidance, in view of the unknown nature and concentration of surface active contaminants in industrial units.

EXPERIMENTAL APPARATUS AND PROCEDURE

Materials

One dispersed phase resistance-controlled and one continuous phase resistance-controlled system were selected for analysis. The former consisted of the solute, acetic acid, (Baker Analyzed Reagent with a residue after evaporation of 0.0008%) diffusing from drops of chlorobenzene (Baker Analyzed Reagent with a boiling range of 405.1 ± 0.6°K) into once-distilled water. The latter system consisted of acetic acid diffusing from drops of distilled water into toluene (Baker Analyzed Reagent with a boiling range of 383.7 ± 1.0°K).

Two surface active agents were placed, in turn, in the aqueous phase of each system. The anionic surfactant, dodecyl sodium sulfate 1 (DSS1), and the cationic surfactant, dodecyl pyridinium bromide (DPB), were both purchased from Distillation Products Industries.

Apparatus

The general layout resembled that shown in figure 1 of the paper by Skelland and Minhas (*81*). To obtain a constant head, a 100 cm³ buret was provided with a tightly fitting rubber stopper through which passed a 4 mm O.D. pyrex tube to admit a slow stream of air to a point within the dispersed phase in the buret. The flow rate of the dispersed phase was controlled by a manostat teflon needle valve fitted with a circular scale and a pointer.

The delivery end of the buret was blown into a glass bulb of approximately 1.906 cm diameter. The lower side of the bulb was drawn into three legs lying on the corners of a 1.906 cm equilateral triangle. These legs were constructed from 5mm I.D. pyrex glass tubing and each was 14 cm long. A ground glass ball fitting was attached to each leg, enabling nozzle attachment via a ball and socket joint. This three-nozzle dispersion system represented an attempt to simulate the hole distribution and multidrop formation conditions on a perforated plate. The plane coalescence area per droplet stream was also about the same as in a commercial column (*59, 60*). The pyrex nozzles were selected carefully because it was found that minor variations in the grinding of the nozzle tips caused drastic changes in the dispersed phase flow rate. The main criterion for nozzle selection was matching drop formation times for a range of settings of the inlet needle valve. The average nozzle tip I.D. for the four systems studied are listed in Table 1.

The extraction columns for both two- (formation and fall) and three-stage (formation, fall, and coalescence) runs were constructed from 5.08 cm I.D. pyrex glass. Both columns were lengthened by attaching sections of 5.08 cm I.D. pyrex glass pipe with aluminum flanges and a teflon gasket. At the foot of each column was a conical section. The two-stage column had a narrow exit tube of approximately 12 cm length and 9 mm I.D. attached to the conical section. By maintaining the level of the liquid-liquid interface in the narrow exit tube, mass transfer during coalescence was minimized because of the large reduction in coalescence area (*8*). The position of the liquid-liquid interface for both types of column was maintained by adjusting a manostat teflon needle valve in the exit tube.

Procedure

Great care was taken to avoid contamination of the apparatus by foreign substances. To remove surfactants from the extraction column and dispersion nozzles, these parts were rinsed with hot chromic acid and distilled water before each experimental run.

The nozzle tips were immersed approximately 5 mm in the continuous phase and the run was initiated by positioning the feed needle valve and starting the stop watch. A second stop watch was used to measure the formation time of either 5 or 10 drops from each nozzle several times during the run.

For the two-stage runs the extraction column exit valve was positioned to maintain the liquid-liquid interface at a marked point in the narrow exit tube. For the three-stage runs the level of the dispersed phase was allowed to build up in the cone at the foot of the column. When the position of the interface reached the top of the cone, the outlet needle valve was opened to drain off the dispersed phase at a rate that kept the interface just above the cone.

At the end of the run the remaining dispersed phase was drained off through the exit needle valve. The continuous phase, after being mixed thoroughly in a separating funnel, was volumetrically analyzed for the total amount of acetic acid transferred during the run. The dispersed phase concentration was not analyzed in this study.

The temperature of the continuous phase was recorded with a mercury-in-glass thermometer and was maintained in the range 298.1 ± 2°K.

The droplet fall velocities were determined by timing the fall through a distance of 30.75 cm, the top mark being approximately 5 cm below the nozzle tip.

For each drop formation time and concentration of surfactant experimental runs were made for at least four different heights of fall.

Organic phase titrations were performed with solutions of potassium hydroxide and ethyl alcohol and aqueous phase titrations used aqueous sodium hydroxide.

Physical properties were measured at 298°K and, with the exception of interfacial tension, all measurements were made in the absence of surfactants. Measurements were always made

Table 1. Nozzle Sizes

	System	Lower barrel I.D. at tip, cm
(1)	HAc—C_6H_5Cl—H_2O—DSS1	0.2360
(2)	HAc—C_6H_5Cl—H_2O—DPB	0.2360
(3)	HAc—H_2O—$C_6H_5CH_3$—DSS1	0.2357
(4)	HAc—H_2O—$C_6H_5CH_3$—DPB	0.2217

Table 2. Physical Properties of Experimental Systems at 298°K

System	$\rho_d \times 10^{-3}$ Kg/m³	$\rho_c \times 10^{-3}$ Kg/m³	μ_d Kg/m-s	μ_c Kg/m-s	$D \times 10^9$ m²/s
H_2O-acetic acid-toluene	1.013	0.8669	0.001066	0.00056	2.265
H_2O-acetic acid-chloro-benzene	1.1005	0.9907	0.000755	0.000876	2.072

on the dispersed and continuous phases as they would exist at the start of each mass transfer experiment, with acetic acid present only in the dispersed phase. Results are reported in Table 2. Interfacial tension values (shown in Figure 1) were obtained from a Model K8600 Du Nöuy Interfacial Tensiometer, accurate to 0.1 mN/m. Viscosities were measured (*39, 40*) with an Ostwald-Fenske type capillary tube viscometer. The dispersed phase density of the HAc—H_2O—C_6H_5Cl system was measured (*39*) with a pycnometer and the density of the aqueous acetic acid solution was evaluated (*40*) with a Westphal Balance. The continuous phase densities were obtained from the literature (*61*).

The experimental value of the liquid diffusion coefficient of acetic acid in toluene at 298°K (2.265×10^{-9} m²/s) has been reported by Chang and Wilke (*62*). The diffusivity of acetic acid in chlorobenzene (2.072×10^{-9} m²/s) was determined from the King, Hsueh, and Mao correlation (*63*).

COMPUTATIONAL PROCEDURE

The individual mass transfer coefficients during drop formation, free fall, and coalescence were isolated from the experimental data using somewhat complex computational procedures developed and reported elsewhere by Minhas (*39, 64, 81*) for the disperse phase and by Hemler (*40, 64*) for the continuous phase.

The individual coefficients during drop formation are based on the surface area of a sphere having the same volume as the drop at detachment. The coefficients during free fall are defined in terms of the surface of an oblate spheroid having the same volume as that of the falling drop (*82*). The total mass transfer from all three droplet streams during coalescence is described in terms of dispersed and continuous phase coefficients based on the plane area of the interface of the coalesced layer with the continuous phase.

DISCUSSION OF EXPERIMENTAL RESULTS

A total of 431 experimental runs was performed (206 for the dispersed resistance-controlled system and 225 for the continuous phase resistance-controlled system). The data have been tabulated elsewhere (*64*).

In several cases, results were compared with theoretical predictions which make no allowance for effects of S.A.A.

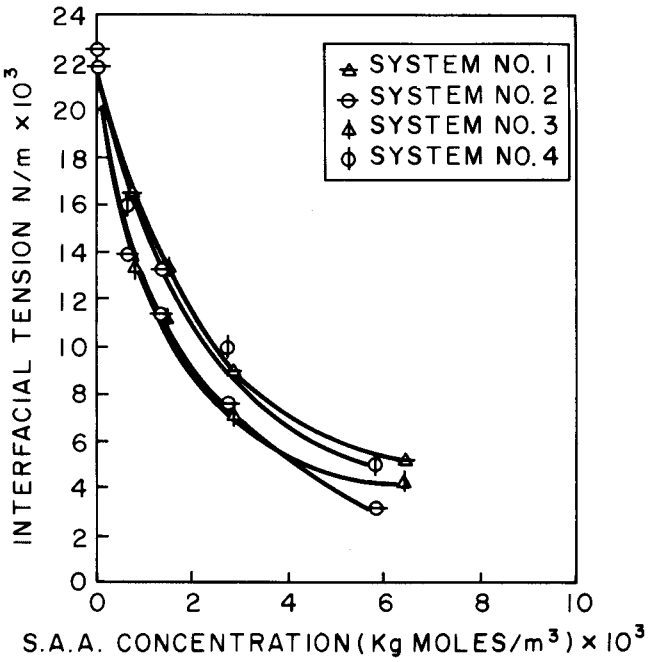

Fig. 1. Effect of S.A.A. concentration on interfacial tension at 298°K

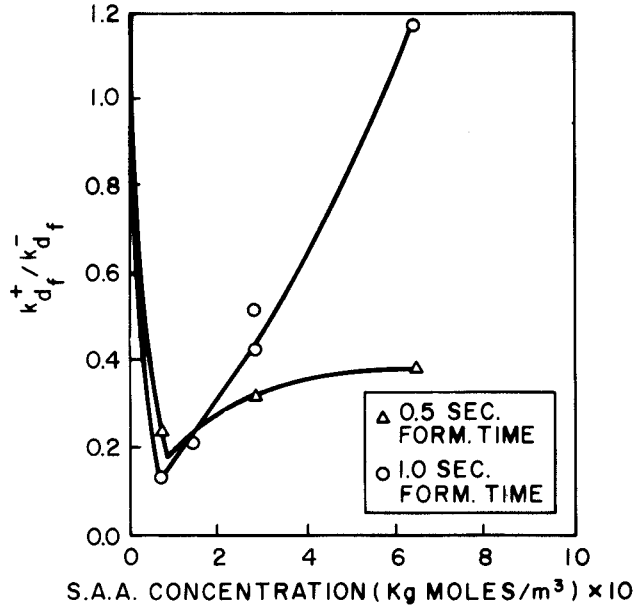

Fig. 2. Effect of S.A.A. on dispersed phase transfer coefficient during drop formation for the system (1) HAc-C_6H_5Cl-H_2O-DSS1.

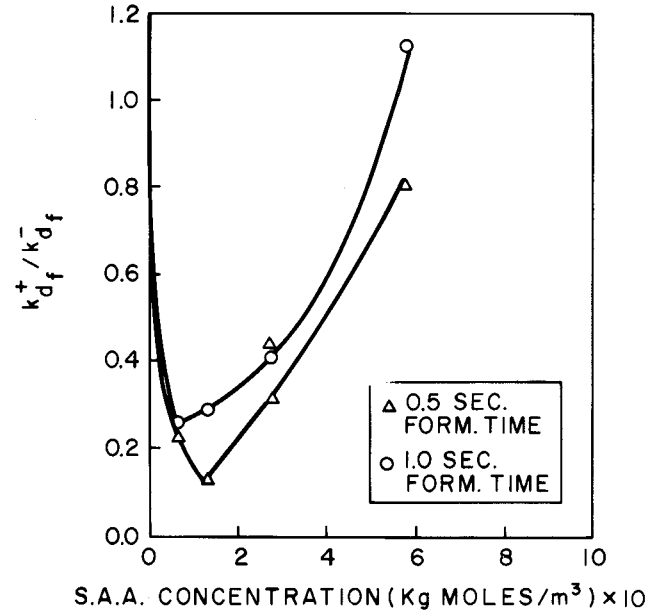

Fig. 3. Effect of S.A.A. on dispersed phase mass transfer coefficient during drop formation for the system (2) HAc-C_6H_5Cl-H_2O-DPB.

Correlation could not, therefore, be expected, but it was felt that order-of-magnitude comparisons might be of some interest.

Dispersed Phase Mass Transfer Coefficients During Drop Formation

The importance of the formation effect for dispersed phase resistance-controlled systems is emphasized by the fact that the fraction of the total mass transfer occurring during formation varied between 0.124 and 0.862 for system (1) and between 0.232 and 0.733 for system (2).

A representation of the effect of surfactants on $k^-_{d_f}$ is illustrated in Figures 2 and 3. The ratio of $k^+_{d_f}$ (with surfactant present) to $k^-_{d_f}$ (dispersed phase formation coefficient without surfactant, as predicted by the Minhas (*39, 81*) correlation, Equation (1)) has been plotted as a function of bulk aqueous phase concentration of surfactant.

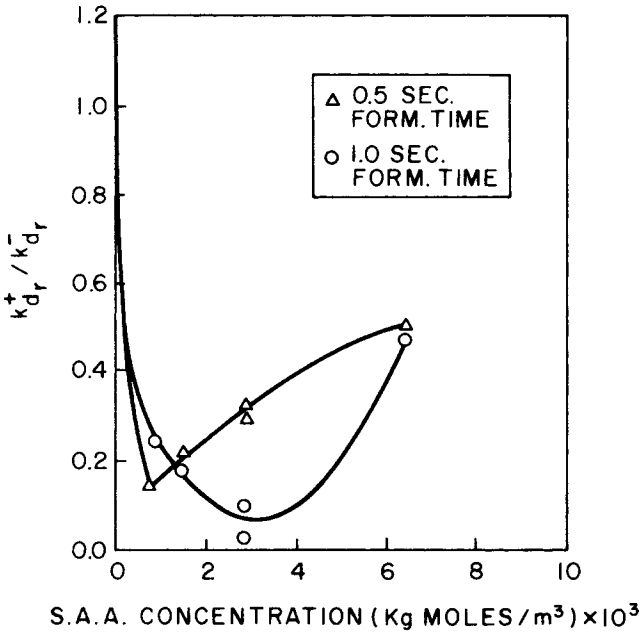

Fig. 4. Effect of S.A.A. on dispersed phase transfer coefficient during drop free-fall for the system (1) HAc-C_6H_5Cl-H_2O-DSS1.

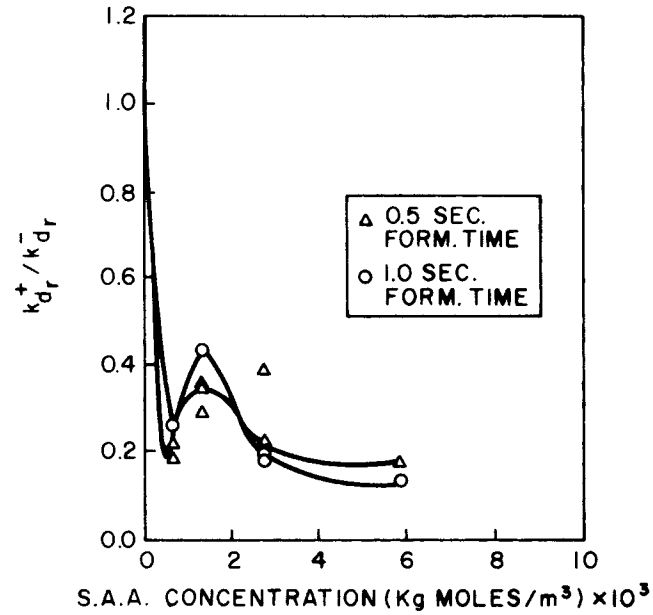

Fig. 5. Effect of S.A.A. on dispersed phase transfer coefficient during drop free-fall for the system (2) HAc-C_6H_5Cl-H_2O-DPB.

$$N_{M1} = 0.0432\, N_{Fr}^{0.089}\, N_T^{-0.334}\, N_{Oh}^{-0.601} \qquad (1)$$

Observed mass transfer rates during drop formation were compared with several theoretical models which, however, make no allowance for the presence of surface active agents (*30* to *32*, *35*). The purpose was merely to obtain order-of-magnitude comparisons. In order to make a comparison, the experimental values of $k^+_{d_f}$ had to be recalculated on the basis of the concentration driving force present in the drop at the start of the formation process. With the exception of the Heertjes model [Equation (2)] [standard deviation = 0.6586 and average absolute % error = 33.73 (±)] the observed mass transfer rate was higher than the theoretically predicted values, which in any event do not follow such observations as the minima in $k^+_{d_f}$. [*The + and − signs in parentheses after each %* error, both here and in the following sections, show that the model in question respectively overestimated (+), underestimated (−), or ran roughly through the middle (±) of most of the points in a given set of experimental data].

$$N_{M1} = (3.429/\sqrt{\pi})\, N_T^{-0.5} \qquad (2)$$

This higher experimental rate may be attributed to the fact that none of the models include mass transfer during drop detachment. Most of the scatter can be explained by noting that the models consider only the effect of varying formation time and diffusivity. Parameters such as density, viscosity, equivalent drop diameter, nozzle velocity, interfacial tension, and concentration of surfactant may also affect the value of $k^-_{d_f}$.

Dispersed Phase Mass Transfer Coefficients During Drop Free-Fall

The effect of the surfactants on $k^-_{d_r}$ is illustrated in Figures 4 and 5. The ratio of $k^+_{d_r}$ (with surfactant present) to $k^-_{d_r}$ [free-fall mass transfer coefficient without surfactant, as predicted by the Skelland and Wellek (*48*) correlation for nonoscillating drops, Equation (3)] has been plotted as a function of bulk aqueous phase concentration of surface active agent.

$$N_{Sh} = 31.4 \left(\frac{4\, D_d\, t_r}{D_e^2} \right)^{-0.34} N_{Sc}^{-0.125}\, N_{We}^{0.37} \qquad (3)$$

The coefficients $k^+_{d_r}$ in the above analysis were calculated only for fall heights in the range 14.0 to 15.0 cm. A specific fall height was chosen in order that the effect of this variable could be eliminated during the analysis of the effect of the surfactants.

It must be pointed out that Figures 4 and 5 agree directionally with the findings of Garner and Skelland (*5*). For the anionic surfactant DSS1 they attribute the initial drastic decrease to stopping of internal drop circulation and to the existence of some interfacial obstruction to transfer which builds up at the interface. The increase after the minimum is attributed to increasing oblateness of the drops due to a reduction in interfacial tension. For the cationic surfactant DPB they again attribute the initial drastic decrease to a retardation of internal circulation. They hypothesize that the increase after the minimum is due to increased oblateness and oscillation of the drops. After a secondary maximum, additional surfactant retards circulation to such an extent that this overrides the effect of increased oblateness and oscillation.

Dispersed Phase Mass Transfer Coefficients During Drop Coalescence

The importance of the coalescence stage for dispersed phase resistance-controlled systems is emphasized by the experimental findings that with surfactants present the fraction of total mass transfer occurring during drop coalescence varied between 0.057 and 0.621 for system (2) and between 0.071 and 0.736 for system (1).

A representation of the effect of the surfactants on $k^-_{d_c}$ is illustrated in Figures 6 and 7, where the ratio of $k^+_{d_c}$ (with surfactant present) to $k^-_{d_c}$ [the dispersed phase coalescence coefficient without surfactant, as predicted by the Minhas (*39*, *81*) correlation, Equation (4)] has been plotted as a function of bulk aqueous phase concentration of S.A.A.

$$N_{M1} = 0.1728\, N_{Sc}^{-1.115}\, N_{Bo}^{1.302}\, N_6^{0.146} \qquad (4)$$

Observed mass transfer rates during drop coalescence were compared with those predicted by the Johnson and

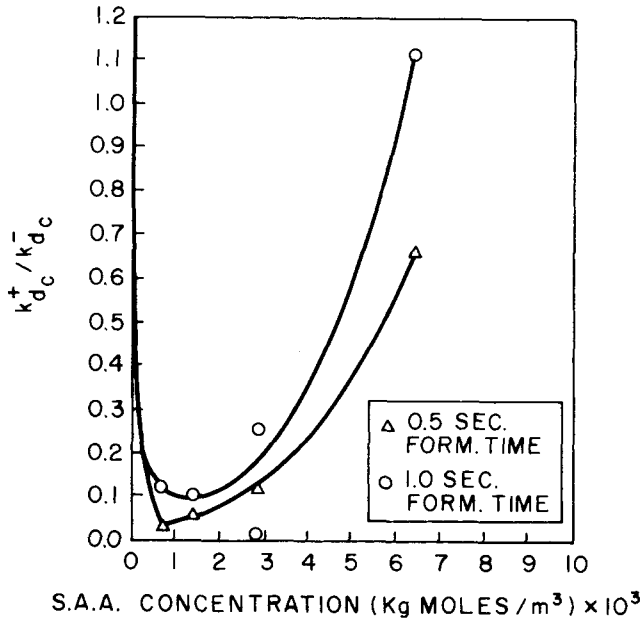

Fig. 6. Effect of S.A.A. on dispersed phase mass transfer coefficient during drop coalescence for the system (1) HAc-C_6H_5Cl-H_2O-DSS1.

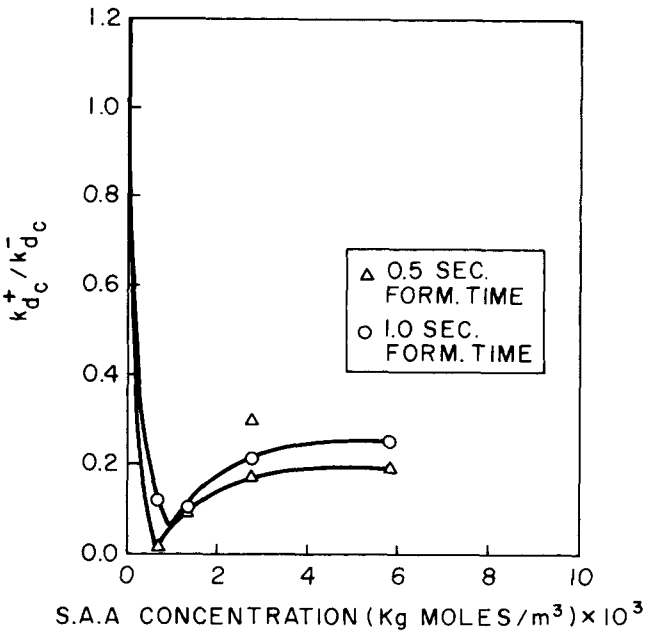

Fig. 7. Effect of S.A.A. on dispersed phase mass transfer coefficient during drop coalescence for the system (1) HAc-C_6H_5Cl-H_2O-DPB.

Hamielec (*38*) adaptation of the Penetration Theory without allowance for surfactants [Equation (5)].

$$N_{M1} = \frac{2.0}{\sqrt{\pi}} N_T^{-0.5} \qquad (5)$$

In order to make a comparison, the experimental value of $k^+_{d_c}$ had to be recalculated on the basis of the concentration driving force present in the drop at the start of the coalescence period. It can be concluded that the Penetration Theory (which postulates that mass transfer occurs at the interface for time t_F, after which another batch of drops arrives and forms a fresh layer) crudely predicts $k^+_{d_c}$ values in a gross sense [standard deviation = 0.4388 and average absolute % error = 59.46 (+)] but the theory does not follow such observed phenomena as the minima in Figures 6 and 7.

Continuous Phase Mass Transfer Coefficients During Drop Formation

The importance of the formation stage for continuous phase resistance-controlled systems is emphasized by the experimental findings that with surfactants present the fraction of total solute transfer occurring during drop formation varied between 0.149 and 0.518 for system (3) and between 0.196 and 0.441 for system (4).

The effect of the surfactants on k^-_{cf} is illustrated in Figures 8 and 9. The ratio of k^+_{cf} (with surfactant present) to k^-_{cf} [calculated from the Hemler (*40*) correlation, Equation (6), for formation without surfactant] has been plotted as a function of the surfactant in the aqueous phase.

$$N_{M2} = 0.3863\, N_{15}^{-0.407}\, N_{16}^{0.148} \qquad (6)$$

It is concluded that the anionic surfactant DSS1 has only a small effect on the value of k^-_{cf}, but the effect of the cationic surfactant DPB is much more drastic, as indicated by Figure 9.

Observed mass transfer rates during drop formation were compared with those predicted by several theoretical models which do not account for S.A.A. effects (*28 to 32*). With the exception of the modified Heertjes model, Equa-

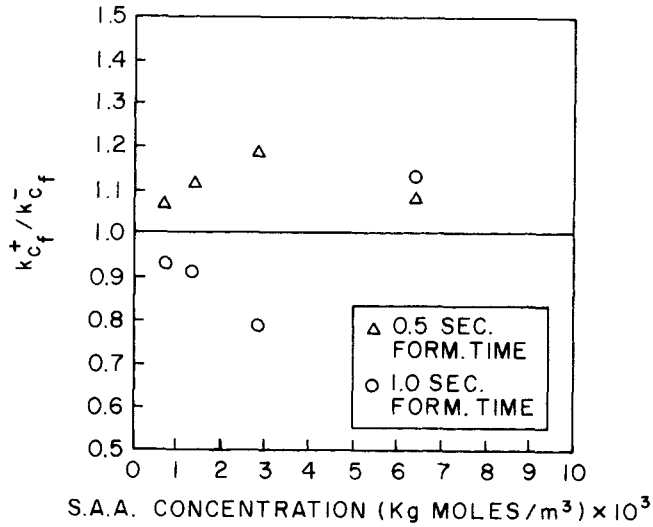

Fig. 8. Effect of S.A.A. on continuous phase mass transfer coefficient during drop formation for the system (3) HAc-H_2O-$C_6H_5CH_3$-DSS1.

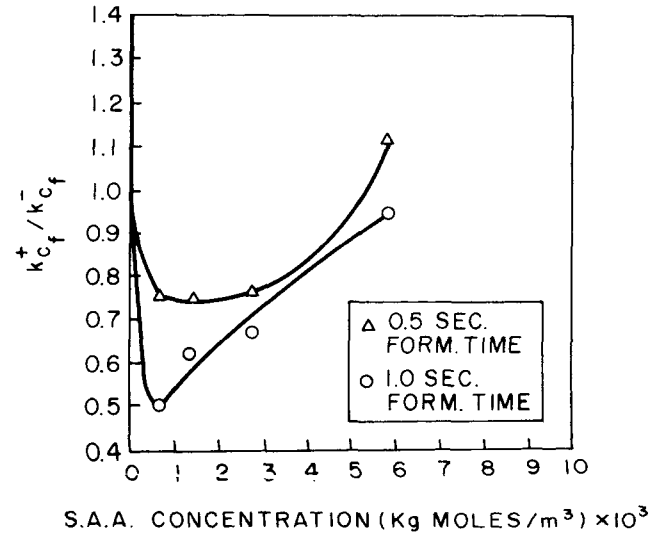

Fig. 9. Effect of S.A.A. on continuous phase mass transfer coefficient during drop formation for the system (4) HAc-H_2O-$C_6H_5CH_3$-DPB.

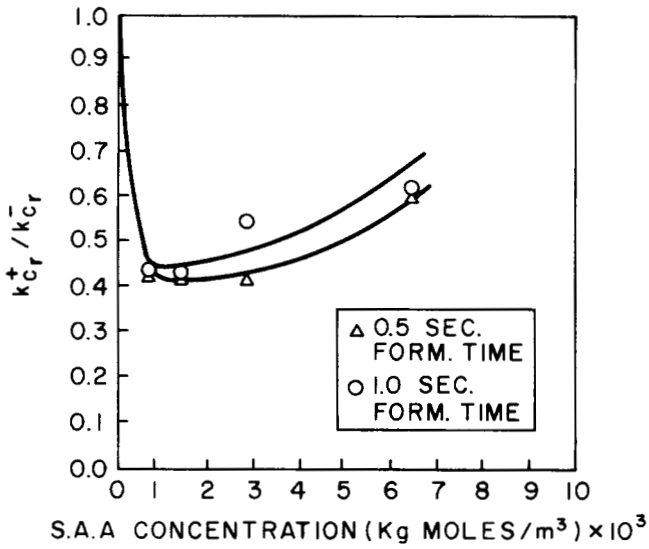

Fig. 10. Effect of S.A.A. on continuous phase mass transfer coefficient during drop free-fall for the system (3) HAc-H_2O-$C_6H_5CH_3$-DSS1.

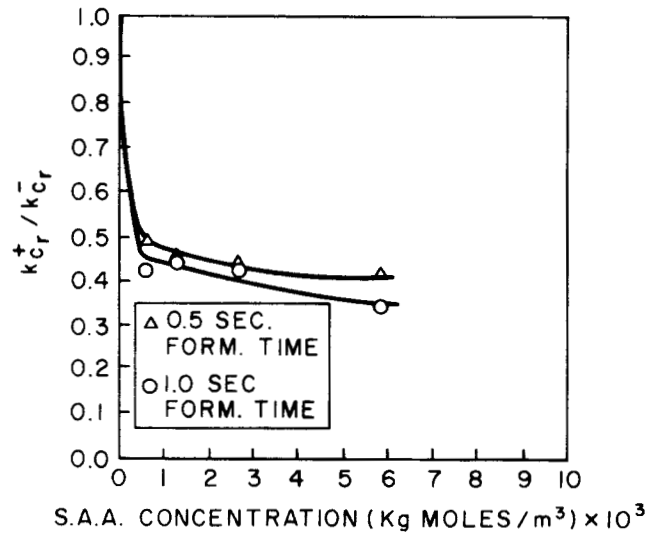

Fig. 11. Effect of S.A.A. on continuous phase mass transfer coefficient during drop free-fall for the system (4) HAc-H_2O-$C_6H_5CH_3$-DPB.

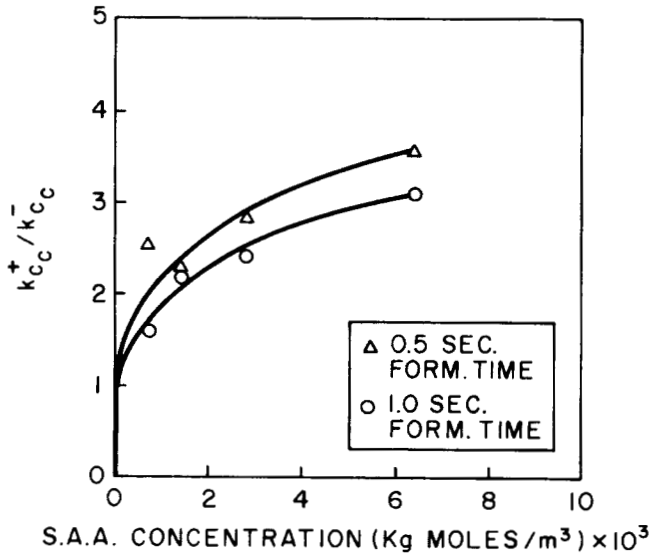

Fig. 12. Effect of S.A.A. on continuous phase mass transfer coefficient during drop coalescence for the system (3) HAc-H_2O-$C_6H_5CH_3$-DSS1.

tion (7), [standard deviation = 1.034 and average absolute % error = 43.95 (−)] the observed mass transfer is considerably higher than the theoretically predicted values.

$$N_{M2} = k_{cf}\,(t_F/D_c)^{0.5} = 1.935 \qquad (7)$$

This higher rate may be attributed to the fact that none of the models include mass transfer during drop detachment. The Heertjes model appears to provide a crude conservative estimate of this mass transfer rate, although the minimum of Figure 9 is, of course, not predicted.

Continuous Phase Mass Transfer Coefficients During Drop Free-Fall

A representation of the effect of surfactants on $k^-_{c_r}$ is illustrated in Figures 10 and 11. The ratio of $k^+_{c_r}$ (with surfactant present) to $k^-_{c_r}$ [calculated from the Hemler (*40*) correlation, Equation (8), for drop free-fall without surfactant] has been plotted as a function of the surfactant in the aqueous phase.

$$\frac{k_{c_r}d_p}{D_c} = 0.915\left(\frac{d_pV_t\rho_c}{\mu_c}\right)^{0.5}\left(\frac{\mu_c}{\rho_cD_c}\right)^{0.5} \qquad (8)$$

Small concentrations of surfactants appear to have a rather drastic effect on the value of $k^+_{c_r}$. System (3) exhibits a minimum value of the coefficient and a rather large increase after the minimum. For system (4) the effect of the surfactant appears to be limiting because $k^+_{c_r}$ approaches a value of approximately four tenths of $k^-_{c_r}$.

Observed mass transfer rates during drop free-fall were compared with those predicted by several theoretical models (*49* to *51*). The Skelland and Cornish (*52*) correlation, Equation (9), was also tested.

$$\frac{k_{c_r}d_p}{D_c} = 0.74\left(\frac{d_pV_t\rho_c}{\mu_c}\right)^{0.5}\left(\frac{\mu_c}{\rho_cD_c}\right)^{0.33} \qquad (9)$$

The Garner and Tayeban correlation for circulating and nonoscillating drops gave a standard deviation of 0.00414. However, the Skelland and Cornish correlation for rigid spheroids is considerably better in the range of the data [standard deviation = 0.00285 and average absolute % error = 38.27 (−)], although it of course does not predict the minimum of Figure 10.

Continuous Phase Mass Transfer Coefficients During Drop Coalescence

The importance of the coalescence end effect for continuous phase resistance-controlled systems is emphasized by the fact that the fraction of total solute transfer occurring during drop coalescence varied between 0.238 and 0.623 for system (3) and between 0.264 and 0.644 for system (4).

The effect of surfactants on $k^-_{c_c}$ is illustrated in Figures 12 and 13. The ratio of $k^+_{c_c}$ to $k^-_{c_c}$ [calculated from the Hemler correlation, Equation (10), for coalescence without surfactant] is plotted against S.A.A. concentration.

$$N_{M4} = 0.000596\,N_{19}^{0.332}\,N_{20}^{0.525} \qquad (10)$$

The most obvious conclusion is that the coefficients with surfactants are significantly greater than the coefficients without surfactant for almost all S.A.A. concentrations. This is contrary to the effect of the surfactants on the previously discussed coefficients $k^-_{d_f}$, $k^-_{d_r}$, $k^-_{d_c}$, $k^-_{c_f}$ and $k^-_{c_r}$.

Observed mass transfer rates during drop coalescence were compared with those predicted by the Johnson and Hamielec (*38*) adaptation of the Penetration Theory without allowance for surfactants [Equation (11)].

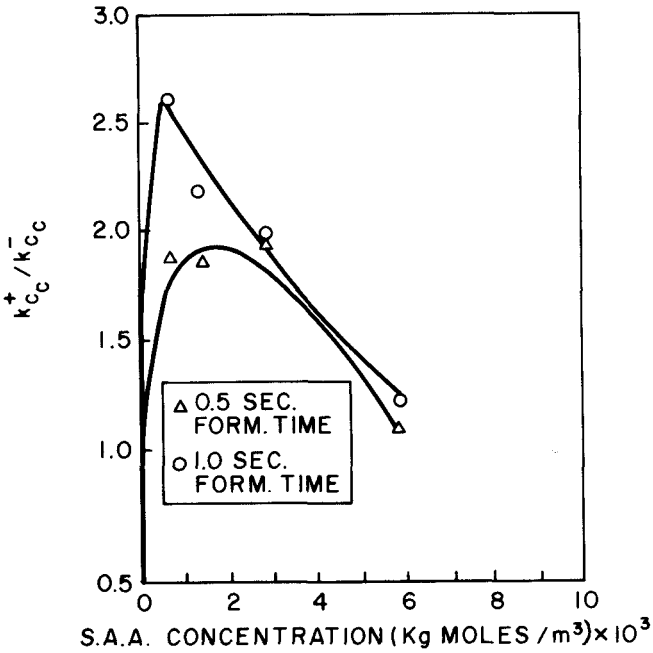

Fig. 13. Effect of S.A.A. on continuous phase mass transfer coefficient during drop coalescence for the system (4) HAc-H_2O-$C_6H_5CH_3$-DPB.

$$k_{cc} = \frac{2}{\sqrt{\pi}} (D_c/t_F)^{0.5} \qquad (11)$$

Predicted and observed orders of magnitude are crudely comparable [standard deviation = 0.000876 and average absolute % error = 27.57 (±)]. However, the shape of Figure 13, for example, is naturally not followed by such predictions.

Licht and Conway (78) and Coulson and Skinner (30) seemingly observed almost the same amount of mass transfer in each of the two end effects (formation and coalescence). (Skelland and Minhas (81), however, show these observations to be fallacious). Treybal (65) earlier used these findings to make the approximation that

$$k_{df}\, a_f = k_{dc}\, a_c \qquad (12)$$

This approximation, when applied to a system with surfactants present, was not verified in the present study because the ratio $k^+_{df}\, a_f/k^+_{dc}\, a_c$ was found to vary in the range 0.131 to 11.072. In the case of the continuous phase, the ratio $k^+_{cf}\, a_f/k^+_{cc}\, a_c$ varied from 0.428 to 1.369.

THE EFFECTS OF FORMATION TIME AND SURFACTANT ON FORMATION AND COALESCENCE COEFFICIENTS

Effects of Formation Time

For a given system, drop size, and concentration of surfactant, a review (39, 64) of existing correlations indicates that the following equation is applicable

$$\frac{k^+}{k^-} = \alpha \frac{{t_F}^{-b}}{{t_F}^{-a}} = \alpha\, {t_F}^{a-b} \qquad (13)$$

The values of "a" obtained from the Minhas and Hemler correlations are presented in Table 3.

The magnitude of "b" is determined by

1. the rigidity of the interface
2. the degree of blocking of the interface by the surface active molecules
3. the speed of migration of the surfactant to the interface

Table 3. Effect of t_F on k^-

Coefficient	a
k^-_{df}	0.666
k^-_{dc}	0.854
k^-_{cf}	0.611
k^-_{cc}	0.500

Table 4. Effect of Formation Time on Ratio of Mass Transfer Coefficient with Surfactant to That Without Surfactant

Coefficient	Surfactant	Effect of t_F on "k ratio" a-b	Effect of increasing t_F	Relevant figure
k_{df}	DSS1	>0	increases k ratio	2
k_{df}	DPB	>0	increases k ratio	3
k_{dc}	DSS1	>0	increases k ratio	6
k_{dc}	DPB	>0	increases k ratio	7
k_{cf}	DSS1	<0	decreases k ratio	8
k_{cf}	DPB	<0	decreases k ratio	9
k_{cc}	DSS1	<0	decreases k ratio	12
k_{cc}	DPB	>0	increases k ratio	13

4. the interaction between surface active agent, solvent, and solute
5. the presence around the drop of interfacial tension gradients which might promote interfacial movement.

Table 4 describes the effect of formation time on the ratio of the mass transfer coefficient with surfactant to that without surfactant.

Both k^+ and k^- vary with t_F raised to a negative exponent. Whether the "k ratio" increases or decreases with increasing t_F merely depends on the relative magnitude of "a" and "b".

One can argue that if the S.A.A. suppresses internal circulation and motion, the mass transfer mechanism would approach unsteady state diffusion as described by the Penetration and other theories for which $b = 1/2$. Therefore, from an examination of Table 3 for this limiting case, the "k ratio" should increase with formation time for at least three of the four coefficients tabulated. This argument is experimentally verified by k_{df} (DSS1 and DPB), k_{cc} (DPB), and k_{dc} (DSS1 and DPB) data.

The directional effect of formation time on k_{cf} (DSS1 and DPB) and k_{cc} (DSS1) is in opposition to the above argument. This is explained later for k_{cc} (DSS1) but is not fully understood in the case of the two k_{cf} plots. It may be that increasing formation time enables the surfactant molecules to rearrange themselves at the interface in such a manner as to more effectively oppose transfer of solute molecules, in accordance with the factors listed above as determining the magnitude of "b".

Effects of Surface Active Agents

Surfactants may reduce mass transfer in several ways, involving

1. interfacial blockage
2. interactions with transferring solute molecules
3. hydrodynamic modifications, such as reducing circulation and oscillation during drop formation and free-fall, and wave modification at the coalescence interface
4. suppression of interfacial turbulence and the Marangoni effect.

On the other hand, surfactants might promote mass transfer by

1. increasing the surface area due to droplet elongation and oblateness during formation and free fall respectively,
2. retarding droplet coalescence at the plane interface,

in the manner established by Hartland (85) and by Lang and Wilke (87). The total transfer surface in the coalescence region is then that of the plane interface plus the surface of those drops waiting to coalesce. The effect could be partially offset by an excessive pile-up of uncoalesced drops, which may reduce the transfer rate. This results from reduction in the concentration gradients due to mutual interference from adjacent spheroids, as described by Cornish (86),

3. enhancing the diffusivity in media structured by the presence of colloidal micelles, in a way analogous to that observed in some non-Newtonian systems (66 to 68, 79, 80). This would require conditions of temperature and concentration conducive to micelle formation (75). Whether or not enhancement of the diffusivity would occur is presently a matter for speculation; some conflicting reports have appeared in certain non-Newtonian studies (83, 84, 88).

Many of the present results exhibit a dramatic reduction in the mass transfer coefficient with increasing S.A.A. concentration. A notable feature is the frequent occurrence of a minimum in the coefficient at S.A.A. concentrations which are much less than the bulk values corresponding to interfacial saturation in static systems (Figure 1). These observations appear in Figures 2 to 7 and 9 to 11. Such minima have been observed in two other types of situation in the presence of surfactants:

1. in mass transfer from falling drops (3, 5, 12), where the increase in the coefficient beyond the minimum was accounted for in terms of increased oblateness and drop oscillations with decreasing interfacial tension,

2. in mass transfer across plane interfaces between two stirred liquids in diffusion cells [Gordon and Sherwood (69) as examined by Garner and Hale (3); also Davies (70) and Davies and Rideal (77)].

In the latter case, variations in size of the interface could not be invoked to explain the minimum, although no minimum was found in the absence of stirring.

The present findings represent the first time that a minimum in the transfer coefficient with increasing concentration of surfactant has been observed in the case of drop formation and coalescence—similar studies have not previously been made.

Explanations have been sought for this minimum; according to J. T. Davies (71) the explanation is still not clear, but he suggests that the reason may be similar to that governing damping of waves by surfactants (72). This refers to the optimum concentration of soluble surface active agent often found to give maximum damping of waves on a free liquid surface; increase or decrease in concentration of S.A.A. about this optimum value leads to considerable intensification of rippling (13, 73, 74).

In the case of k_{cc} (Figures 12 and 13) a substantial increase in the transfer coefficient is observed when the surfactants are present, that is, the 'k ratio' is greater than one. The solubility of DSS1 and DPB in toluene at the prevailing temperature was too low to permit micelle formation. However, visual observation showed that retarded coalescence with increasing S.A.A. concentration was significantly greater in the case of both toluene systems than for the chlorobenzene systems. The effect was greatest in the system of Figure 13, for which more than one layer of uncoalesced drops was seen at the plane interface at the higher concentrations of DPB. Shorter drop formation times also increased the number of uncoalesced drops at the interface at any instant. For a typical drop diameter of 0.6 cm, 18 uncoalesced drops (or about 1/3 of a single close-packed layer) are sufficient to double the mass transfer surface in the coalescence region. Thus various fractions (≤ 0.865) of a single close-packed layer of uncoalesced drops would provide enough additional transfer surface to account for all the increased $k^+{}_{cc}$ values in Figure 12, neglecting the effects of droplet interaction (86). The larger number of uncoalesced drops at $t_F = 0.5$ sec for a given DSS1 concentration causes the curve for $t_F = 0.5$ sec to lie above that for $t_F = 1.0$ sec.

In Figure 13, increased surface due to retarded coalescence again prevails in increasing the total transfer (and hence $k^+{}_{cc}$) at low concentrations of DPB. At higher concentrations, excessive pile-up of uncoalesced drops—forming more than one layer—was observed. This may have reduced the transfer rate [because of interacting effects of adjacent 'spheres' (86)] enough to outweigh the effects of further increase in the surface. These considerations could explain the maxima in Figure 13. For a given concentration of DPB, droplet pile-up at the interface was more severe at the shorter formation time. Reduction in transfer rate at higher DPB would be correspondingly more pronounced for $t_F = 0.5$ sec, so that the curve for this t_F lies below that for $t_F = 1.0$ sec.

In the case of k_{dc} (Figures 6 and 7) reductions in the coefficient ratio were found at all concentrations of S.A.A. It can only be assumed that the balance of effects was strongly in favor of those factors listed earlier (1 to 4) which tend to reduce transfer rates when surfactants are present. The minimum $k^+{}_{dc}/k^-{}_{dc}$ ratio found in this case might also be related to an optimal concentration of S.A.A. which minimizes rippling of the coalescence surface in a way analogous to that noted earlier for free surfaces (13, 72 to 74). The surface renewal rate would consequently be minimized, leading to a minimal value of the transfer coefficient.

A balance between those factors tending respectively to decrease and to increase transfer appears to be highly specific with regard to system, surface active agent concentration, and hydrodynamic process (drop formation, free-fall, or coalescence) involved.

NOTATION

a = exponent defined in Equation (13)
a_c = coalescence area/droplet stream, cm²
a_f = surface area of spherical drop at detachment, cm²
b = exponent defined in Equation (13)
D, D_c, D_d = diffusivity, in the continuous and disperse phase, m²/s
D_e = equivalent drop diameter, m
d_p = total surface area of a spheroidal drop divided by the perimeter normal to flow, m
g = acceleration due to gravity, m/s²
k_{cc}, k_{dc} = continuous and dispersed phase individual mass transfer coefficients during coalescence, m/s
k_{cf}, k_{df} = continuous and dispersed phase individual mass transfer coefficients during formation, m/s
k_{cr}, k_{dr} = continuous and dispersed phase individual mass transfer coefficients during free-fall, m/s
$N_6 = V_t^2 t_F/D_d$
$N_{15} = (\rho_d - \rho_c)\, g t_F \mu_c/\rho_c \sigma_c g_c$
$N_{16} = g t_F^2/D_e$
$N_{17} = D_e V_t/D_c$
$N_{18} = \rho_c V_t^4/g\sigma_c g_c = N_{Fr} \times N_{We}$
$N_{19} = V_t^3 \rho_c/g\mu_c$
$N_{20} = D_e^2 V_t^3\, \rho_c\rho_d/\mu_d\, \sigma_c\, g_c = N_{We} \times N_{Red}$
$N_{Bo} = (\rho_d - \rho_c)\, g\, D_e^2/\sigma_c\, g_c$, Bond Number
$N_{Fr} = V_n^2/D_e\, g$, Froude Number

N_{M1} = $k_{df}\ t_F/D_e$ [Equations (1) and (2)], $k_{dc}\ t_F/D_e$ [Equations (4) and (5)]
N_{M2} = $k_{cf}\ (t_F/D_c)^{0.5}$
N_{M3} = $k_{cr}\ D_e/D_c$
N_{M4} = $k_{cc}\ (t_F/D_c)^{0.5}$
N_{Oh} = $\mu_d/(\rho_d D_e\ \sigma_c\ g_c)^{0.5}$
N_{Sc} = $\mu/\rho\ D$, Schmidt Number
N_{Sh} = $k_{dr}\ D_e/D$, Sherwood Number
N_{Red} = $V_t D_e\ \rho_d/\mu_d$
N_{Rec} = $V_t De\ \rho_d/\mu_c$
N_T = $D_e^2/t_F D_d$, time group
N_{We} = $\rho_c V_t^2 D_e/\sigma_c g_c$, Weber Number
t_r = time of free-fall, s
t_F = time of drop formation, s
V_n = nozzle velocity, m/s
V_t = terminal velocity of drop, m/s

Greek Letters

α = proportionality constant
ρ, ρ_c, ρ_d = density, of the continuous and dispersed phase, Kg/m^3
μ, μ_c, μ_d = viscosity, of the continuous and dispersed phase, Kg/m-s
σ_c = interfacial tension at a concentration 'c' of surfactant, N/m

Superscripts

$+$ = with surfactant present
$-$ = without surfactant present

LITERATURE CITED

1. Boye-Christensen, G., and S. G. Terjesen, *Chem. Eng. Sci.*, 7, 222 (1958).
2. *Ibid.*, **9**, 225 (1958).
3. Garner, F. H., and A. R. Hale, *Chem. Eng. Sci.*, **2**, 157 (1953).
4. ———., and A. H. P. Skelland, *ibid.*, **4**, 149 (1955).
5. ———., *Ind. Eng. Chem.*, **48**, 51 (1956).
6. Holm, A., and S. G. Terjesen, *Chem. Eng. Sci.*, **4**, 265 (1955).
7. Jenkins, R., *Heat Transfer and Fluid Mechanics Institute*, Stanford Univ. Press, Palo Alto, Calif. (1951).
8. Lindland, K. P., and S. G. Terjesen, *Chem. Eng. Sci.*, **5**, 1 (1956).
9. West, F. B., A. J. Herrman, A. T. Chong, and L. E. K. Thomas, *Ind. Eng. Chem.*, **44**, 625 (1952).
10. West, F. B., P. A. Robinson, A. C. Morgenthaler, T. R. Beck, and D. K. McGregor, *ibid.*, **43**, 234 (1951).
11. Johnstone, H. F., *Trans. Am. Inst. Chem. Eng.*, **35**, 621 (1939).
12. Farmer, W. S., Oak Ridge National Lab. Unclassified Report, ORNL 635 (1950).
13. Emmert, R. E., and R. L. Pigford, *Chem. Eng. Progr.*, **50**, 87 (1954).
14. Cullen, E. J., and J. F. Davidson, *Chem. Eng. Sci.*, **6**, 49 (1956).
15. Hutchinson, E. J., *J. Phys. Chem.*, **52**, 897 (1948).
16. Lewis, J. B., *Chem. Eng. Sci.*, **3**, 248 (1954).
17. Elzinga, E. R., and J. T. Banchero, *AIChE J.*, **7**, 78 (1961).
18. ———., *Chem. Eng. Progr. Symp. Ser. No. 29*, **55**, 149 (1960).
19. Garner, F. H., and P. J. Haycock, *Proc. Roy. Soc.* **A252**, 457 (1959).
20. Savic, P., Nat. Res. Council Can., Rept. No. MT-22, Ottawa (1953).
21. Baird, M. H. I., and A. E. Hamielec, *Can. J. Chem. Eng.*, **40**, 119 (1962).
22. Garner, F. H., and D. Hammerton, *Chem. Eng. Sci.*, **3**, 1 (1954).
23. Horton, T. J., T. R. Fritsch, and R. C. Kintner, *Can. J. Chem Eng* **43** 143 (1956).
24. Schechter, R. S., and R. W. Farley, *ibid.*, **41**, 103 (1963).
25. Davies, J. T., and E. K. Rideal, *Interfacial Phenomena*, Academic Press, N. Y. (1963).
26. Friedlander, S. K., *AIChE J.*, **3**, 43 (1957).
27. Licht, W., and G. S. R. Narasimhamurty, *ibid.*, **1**, 366 (1955).
28. Licht, W., and W. F. Pansing, *Ind. Eng. Chem.*, **45**, 1885 (1953).
29. Michels, H. H., "The Mechanism of Mass Transfer During Bubble Growth," Ph.D. thesis, Univ. Delaware, Newark (1960).
30. Coulson, J. M., and S. J. Skinner, *Chem. Eng. Sci.*, **1**, 197 (1952).
31. Heertjes, P. M., W. A. Holve, and H. Talsma, *ibid.*, **3**, 122 (1954).
32. Groothuis, H., and H. Kramers, *ibid.*, **4**, 17 (1955).
33. Heertjes, P. M., and L. H. DeNie, *ibid.*, **21**, 755 (1966).
34. Angelo, J. B., E. N. Lightfoot, and D. W. Howard, *AIChE J.*, **12**, 751 (1966).
35. Baird, M. I. H., *Chem. Eng. Sci.*, **9**, 267 (1959).
36. Beek, W. J., and H. Kramers, *ibid.*, **16**, 909 (1962).
37. Ilkovic, D., *Coll. Czech. Chem. Commun.*, **6**, 498 (1934).
38. Johnson, A. I., and A. E. Hamielec, *AIChE J.*, **6**, 145 (1960).
39. Minhas, S. S., Ph.D. thesis, Univ. Notre Dame, Ind. (1969).
40. Hemler, C. L., *ibid.* (1973).
41. Newman, A. B., *Trans. Am. Inst. Chem. Engrs.*, **27**, 203 (1931).
42. Vermeulen, T., *Ind. Eng. Chem.*, **45**, 1664 (1953).
43. Grober, H., *Z. Ver. deut. Ing.*, **69**, 705 (1925).
44. Kronig, R., and J. C. Brink, *Appl. Sci. Res.*, A-2, 142 (1950).
45. Higbie, R., *Trans. AIChE*, **31**, 365 (1935).
46. Handlos, A. E. and Baron, T., *AIChE J.*, **3**, 127 (1957).
47. Wellek, R. M., and A. H. P. Skelland, *ibid.*, **11**, 557 (1965).
48. Skelland, A. H. P., and R. M. Wellek, *ibid.*, **10**, 491 (1964).
49. Frossling, N., *Gerlands Beitr. Geophysik*, **52**, 170 (1938).
50. Garner, F. H., and M. Tayeban, *Anal. Real Soc. Espan. Fisica y Quim., Ser. B—Quim. Tomo LVI*, **8**, 479 (1960).
51. Boussinesq, J. J., *Math, Pures et appliques*, Ser. 6, **1**, 285 (1905).
52. Skelland, A. H. P., and A. R. H. Cornish, *AIChE J.*, **9**, 73 (1963).
53. Huang, W. S., and R. C. Kintner, *ibid.*, **15**, 735 (1969).
54. Lochiel, A. C., *Can. J. Chem. Eng.*, **43**, 40 (1965).
55. Chao, B. T., *Phys. Fluids*, **5**, 69 (1962).
56. Davies, J. T., *Proc. Roy. Soc.* **A290**, 515 (1966).
57. Levich, V. G., *Z. fiz. Khim.*, **22**, 727 (1948).
58. Levich, V. G., *Physiochemical Hydrodynamics*, (Eng. Transl.), Prentice-Hall, Englewood Cliff, N. J. (1962).
59. Treybal, R. E., *Mass Transfer Operations*, 1st. ed., p. 378, McGraw-Hill, N. Y. (1955).
60. Treybal, R. E., and F. E. Dumoulin, *Ind. Eng. Chem.*, **34**, 710 (1942).
61. *Handbook of Chemistry and Physics*, 48th ed., The Chemical Rubber Co. (1967).
62. Chang, P., and C. R. Wilke, *J. Phys. Chem.*, **59**, 592 (1955).
63. King, C. J., L. Hsueh, and K. W. Mao, *J. Chem. Eng. Data*, **10**, 348 (1965).
64. Caenepeel, C. L., Ph.D. thesis, Univ. Notre Dame, Ind. (1970).
65. Treybal, R. E., Liquid Extraction, 2nd. ed., p. 471, McGraw-Hill (1963).
66. Metzner, A. B., *Nature*, **208**, 267 (1965).
67. Astarita, G., *Ind. Eng. Chem. Fundamentals*, **4**, 236 (1965).
68. Ponter, A. B., and G. A. Davis, *Nature*, **210**, 837 (1966).
69. Gordon, K. F., and T. K. Sherwood, Am. Inst. Chem. Engrs. Meeting Toronto (1953).
70. Davies, J. T., *Adv. Chem. Eng.*, **4**, 33 (1963).
71. ———., private Communication (1969).
72. ———., and R. W. Vose, *Proc. Roy. Soc.* **A286**, 218 (1965).
73. Tailby, S. R., and S. Portalski, *Trans. Inst. Chem. Engrs.*, **39**, 328 (1961).
74. Kafesjian, R., A. Plank, and E. R. Gerard, *AIChE J.*, **7**, 463 (1961)
75. Schwartz, A. M., and J. W. Perry, *Surface Active Agents*, 1st ed., p. 305, Interscience, N. Y. (1949).

76. Kintner, R. C., *Adv. Chem. Eng.*, **4**, 83 (1963).
77. Davies, J. T., and E. K. Rideal, Interfacial Phenomena, 1st. ed., pp. 318, 335-337, Academic Press, N. Y. (1961).
78. Licht, W., and J. B. Conway, *Ind. Eng. Chem.*, **42**, 1151 (1950).
79. Barlage, W. B., Jr., "Determination of Diffusion Coefficients for gases in Non-Newtonian Fluids under Conditions of Known Shear Rate," Final Report to N.S.F. (grant No. GB-4036) from Clemson Univ. S. C. (1969).
80. Secor, R. M., *AIChE J.*, **11**, 452 (1965).
81. Skelland, A. H. P., and S. Minhas, *ibid.*, **17**, 1316 (1971).
82. Wellek, R. M., A. K. Agrawal, and A. H. P. Skelland, *ibid.*, **11**, 557 (1965).
83. Quinn, J. A., and L. M. Blair, *Nature*, **214**, 907 (1967).
84. Plevan, R. E., and J. A. Quinn, *AIChE J.*, **12**, 394 (1966).
85. Hartland, S., *Trans. Inst. Chem. Engrs.* (London), **46**, T275 (1968).
86. Cornish, A. R. H., *ibid.*, **43**, T332 (1965).
87. Lang, S. B., and C. R. Wilke, *Ind. Eng. Chem. Fundamentals*, **10**, 341 (1971).
88. Osmers, H. R., and A. B. Metzner, *ibid.*, **11**, 161 (1972).

Manuscript received November 15, 1971; revision received June 29, 1972; paper accepted June 30, 1972.

Finite Element Analysis of Two-Dimensional Slow Non-Newtonian Flows

A finite element method is applied to isothermal incompressible two-dimensional slow flows of power-law fluids. Examples considered are rectangular and axisymmetric converging channel flows, recirculating flows in rectangular channels, and flow round cylinders. Results are successfully compared with both finite difference and analytical solutions. The flexibility of finite element methods makes them very suitable for problems involving complex boundary geometries. The method used is particularly suitable for non-Newtonian flows and can treat both rectangular and axisymmetric geometries.

KALIPADA PALIT
and
ROGER T. FENNER

Mechanical Engineering Department
Imperial College of Science and Technology
London S.W.7., England

SCOPE

There are many industrial examples of slow non-Newtonian flows, such as in polymer processing which involves the flow of highly viscous melts in extruders, dies, and moulds. In slow flows, fluid inertia forces are negligible compared to viscous and pressure forces.

Attention is confined to steady incompressible two-dimensional viscous flows in regions whose boundaries are rigid but not necessarily stationary. The flows are two-dimensional in the sense that only velocities in the plane of the problem region are considered, although this does not preclude flow normal to this plane. The flow may be axisymmetric in that the actual three-dimensional flow region is formed by rotating the two-dimensional problem region about some axis of symmetry in the same plane. The examples considered here are flows in both rectangular and axisymmetric converging channels which are typical of polymer extrusion dies, including wire-coating dies. Also considered are recirculating flows in rectangular channels, such as screw extruder channels, and flow round cylinders, such as mixing pins in these channels. The flows are assumed to be isothermal in the sense that temperature variations do not significantly affect the viscous properties of the fluids.

The object of the work described here is to apply finite element (FE) methods to two-dimensional flow problems traditionally solved by finite difference (FD) methods and to demonstrate the advantages of the FE approach. FD methods involve substituting FD approximations for the derivatives contained in the differential conservation equations. These approximations are in terms of the values of the variables at discrete points in the problem region. The points usually lie in rows parallel to the coordinate axes and are frequently, though not necessarily (Gosman et al., 1969) equispaced along these rows. Examples of FD analysis of two-dimensional flow problems include Burggraf (1966), Gosman et al. (1969), and Martin (1969).

FE methods require the problem region to be divided into small subregions, or finite elements. For example, a two-dimensional region may be divided into a mesh of triangles or quadrilaterals. The relevant variables are again required in terms of values at discrete nodal points in the mesh, the corners of the elements (and sometimes additional points on the element boundaries). An appropriate (polynomial) function of position is assumed for each variable within each element. A variational formulation (see, for example, Schechter, 1967) is normally used to solve for the nodal point variables by minimizing appropriate functionals. FE methods are well established in the fields of structural and solid continuum mechanics (see Zienkiewicz, 1971) but have not been widely used in solving fluid mechanics and heat transfer problems. General examples include Martin (1968) and Oden and Somogyi (1969). Atkinson et al. (1969, 1970) applied FE methods to two-dimensional Newtonian flow problems. In a previous paper (Palit and Fenner, 1972) the present authors applied a FE method to non-Newtonian channel flow normal to the plane of the mesh.

Correspondence concerning this paper should be addressed to R. T. Fenner.